COAL PERMEABILITY CHANGE
CAUSED BY MINING-INDUCED STRESS

Lulu ZHANG[1,3], Bo LI[1,3]*, Jianping WEI[1,2,3],
Zhihui WEN[1,3], Yongjie REN[1]

[1] State Key Lab Cultivation Base, Henan Province Key Lab of Gas Geology & Gas Control, Henan Polytechnic University, Jiaozuo, 454003, China

[2] State and Local Joint Engineering Laboratory for Gas Drainage & Ground Control of Deep Mines, Henan Polytechnic University, Jiaozuo, 454003, China

3 Collaborative Innovation Center of Coal Work Safety, Henan Province, Henan Polytechnic University, Jiaozuo, 454003, China

Abstract: To study coal permeability evolution under the influence of mining actions, we conducted a sensitivity index test on permeability to determine the influence of axial and confining stresses on coal permeability. Loading and unloading tests were performed afterward, and the differences between loading and unloading paths in terms of strain and permeability were studied. A permeability evolution model was built in consideration of absorption swelling and effective stress during modeling. An effective stress calculation model was also built using axial and confining stresses. The calculation results of the two models were compared with experimental data. Results showed that permeability were more sensitive to confining stress than axial stress, and effective stress placed a large weight on confining stress. Large axial and radial deformations at peak strength were observed during unloading. In the unloading phase, the permeability of coal began to increase, and the increment was enhanced by large initial axial stress when confining stress was loaded. permeability sensitivity to axial and confining stresses were used to explain these permeability changes. The calculation results of the models fitted the experimental data well. Therefore, the proposed models can be used to calculate effective stress on the basis of axial and confining stresses and describe permeability change in coal under the influence of mining actions.

***Keywords*:** *mining-induced stress; permeability; unloading path; sensitivity index; effective stress*

* Corresponding author: hpulibo@126.com (B Li)

1. INTRODUCTION

The permeability of coal seams is an important parameter in underground mining and presents many applications (Zhang et al. 2017), which include gas drainage system design and ventilation regulation. This parameter also determines the gas content of underground atmosphere, which presents a potential hazard to mining facilities and personnel. Therefore, studying the permeability of coal seams is essential.

Mining activities disturb the original stress state of coal seams and lead to the re-distribution of coal seam stress (Shen et al. 2018). The permeability of coal seams evolves with the change in coal seam stress. Coal in front of a mining face undergoes original stress, stress concentration, and unloading states successively due to the influence of mining activities (Zhang et al. 2017). This process is illustrated in Fig. 1, which shows that stress remains constant in the original stress region, whereas it decreases gradually in the stress unloading region. In the stress concentration region, coal seam is subjected to axial stress from overlying strata, and the roadway and working face around the coal seam provide a certain deformation space that results in the unloading of confining stress. Therefore, loading of axial stress and unloading of confining stress
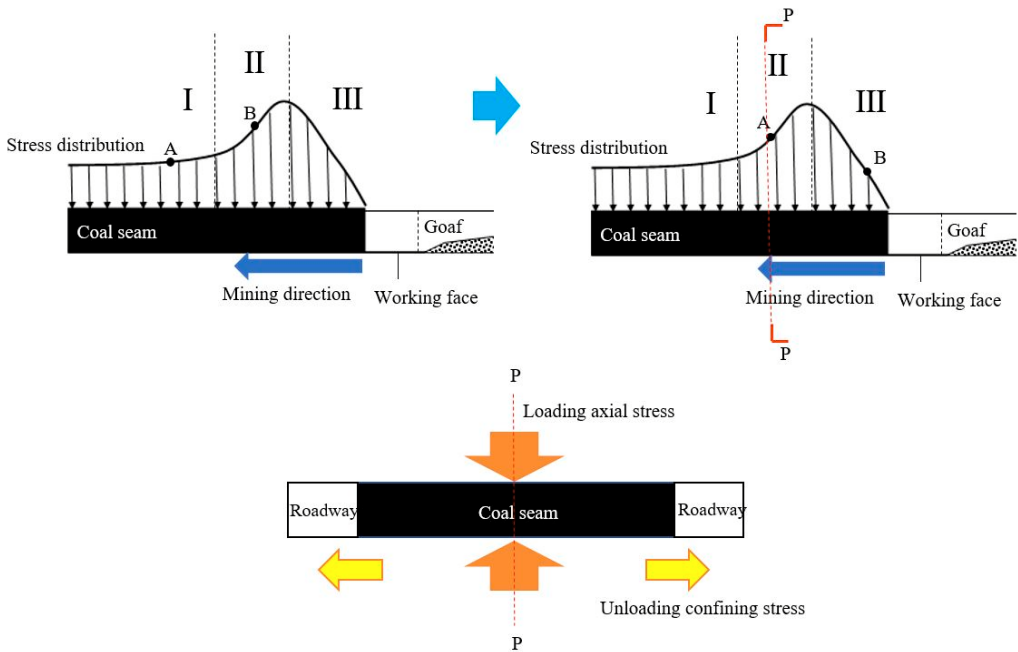

Fig. 1. Stress distribution under the effect of mining actions: I – original stress region,
II – stress concentration region, III – unloading states region

coexist in the stress concentration region, in which the evolution of coal permeability is much more complicated than that in the two other regions.

Many studies have focused on the mechanical characteristics of coal under a conventional loading path (Huang, Liu 2013; Zou et al. 2016; Meng et al. 2015). However, coal deformation differs significantly when loading of axial stress and unloading of confining stress occur simultaneously. Some studies have found that axial and radial strains under unloading conditions are larger than those under loading conditions (Chen et al. 2016a; 2016b), and this situation indicates that coal is deformed more easily by the unloading of confining stress than by the loading of axial stress. Zhao and Wang (2011) discovered that gas pressure influences the change in radial strain during the unloading of confining stress. Several researchers focused on the mechanical properties of coal during unloading. An example is Xie et al. (2011), who designed an unloading path according to different mining conditions and studied the mechanical properties of coal using this unloading path. Huang et al. (2010) also designed different unloading paths and studied the variation law of mechanical parameters during unloading. Permeability during the unloading of confining stress and during conventional loading also exhibits significant differences (Xue et al. 2017). Jiang et al. (2011) studied the influence of different unloading speeds on the mechanism and gas seepage features of coal. In Yin's work, changes in permeability under different unloading modes, including conventional loading, different axial stresses when unloading confining stress, and different unloading rates of confining stress were investigated (Yin et al. 2013). The effect of effective stress on the permeability of raw coal under unloading conditions was also analyzed in Yin's research; permeability increased (Yin et al. 2015) and was negatively related to effective stress (Yin et al. 2014) when confining stress was unloaded.

The strain, mechanical properties, and permeability of coal differ from those during conventional loading when confining stress is unloaded while axial stress is loaded, but studies have failed to provide an explanation for permeability variation under these conditions. In the stress concentration region, a change in axial and confining stresses leads to a change in effective stress (Li et al. 2014), which exerts a significant influence on coal deformation and permeability (Jasinge et al. 2011). Thus, the change in effective stress needs to be considered when studying permeability evolution in the stress concentration region.

In this study, the sensitivity of permeability to axial and confining stresses was investigated. Different unloading paths were designed, and these loading paths were considered when examining the differences in permeability during loading and unloading. These differences were explained by the sensitivity of permeability to axial and confining stresses. A permeability evolution model under unloading paths was also established based on the change in effective stress, and the accuracy of this model was verified using experimental data.

2. METHODS

2.1. TRIAXIAL SEEPAGE EXPERIMENT SYSTEM

The triaxial seepage experiment system utilized in this study was composed of many subsystems, including stress loading system, temperature control system, gas pressure control, coal sample holder, degassing system, and data acquisition device. The stress loading system consisted of two sets of manual operation pumps that produced confining and axial stresses. The temperature control system ensured that the test temperature was constant by using an electric heating coil around the sample holder and automatic temperature regulating device. The accuracy of the temperature control system was ±0.1 °C. The pore pressure control system consisted of high-pressure gas, a pressure reducing valve, and gas lines. A vacuum pump was attached to the end of the experimental system and utilized to degas the experimental system. The data acquisition system consisted of a strain sensor and a gas flowmeter. The strain sensor was used to collect sample strain during the experiment, and the flow meter was utilized to measure the quantity of gas that permeated through the sample. A diagram of the triaxial seepage experiment system is shown in Fig. 2.
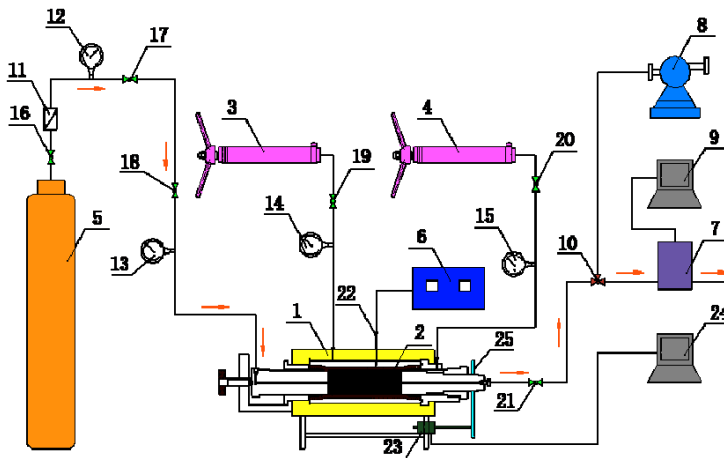

Fig. 2. Diagram of the triaxial seepage experiment system

In Figure 2, No. 1 is the coal sample holder, No. 2 is the coal sample, Nos. 3 and 4 are manual operation pumps, No. 5 is pressured methane, No. 6 is the thermostat, No. 7 is the gas flowmeter, No. 8 is the vacuum pump, Nos. 9 and 24 are computers, No. 10 is the three-way valve, No. 11 is the pressure-reducing valve, Nos. 12 to 15 are pressure gauges, Nos. 16 to 21 are valves, No. 22 is the temperature sensor, No. 23 is the strain sensor, and, No. 25 is the baffle.

Confining and axial stresses were loaded by manual operation pumps (Fig. 2, Nos. 3 and 4) during testing. The valve was turned off (Fig. 2, No. 18), and the vacuum pump was turned on (Fig. 2, No. 8) to degas the system. Then, the valve was turned on (Fig. 2, No. 18). High-pressure methane axially permeated through the coal sample; the methane flow path is denoted by red arrows in Fig. 2. Coal strain and methane flow during this process were automatically recorded by software. The permeability of the coal sample was calculated with Darcy's law (Tiab, Donaldson 2016) and expressed by the following equation.

$$k = \frac{0.2\,p_0\mu LQ}{A(p_i^2 - p_o^2)},$$ (1)

where k is the permeability of the sample in 10^{-15} m^2, p_0 is atmospheric pressure, i.e., 0.1 MPa, μ is the dynamic viscosity of methane, i.e., 11.067×10^{-6} Pa·s, L is sample length, i.e., 10 cm, Q is methane flow in cm^3/s, A is the bottom area of the sample, i.e., 19.625 cm^2; and p_i and p_o are the inlet and outlet pressures, respectively (0.7 and 0.1 MPa).

2.2. SAMPLE PREPARATION

The coal samples used in this experiment were processed by typical anthracite from a mining area in Jincheng, Shanxi Province, China. Fresh blocks of raw coal were selected from the working face. Several of these raw coal blocks were used for basic parameter testing, and the results are shown in Table 1. The rest were prepared into cylindrical samples with 10 cm height and 5 cm diameter.

Coal seams possess bedding planes because of geological action, indicating that coal is anisotropic (Chen et al. 2012). Coal stratification should thus be considered during sample preparation. Coal samples marked with V_1 to V_4 were perpendicular to the stratification to be consistent with the actual situation of the coal seam, but a single sample (marked with P_1) was parallel to the stratification to obtain mechanical parameters. The stratification of coal is shown in Fig. 3. After preparation, the samples were placed in a dry box and dried at 60 °C.

Table 1. Basic parameters of coal samples

Parameters	Value	Unit
Adsorption capacity	42	m^3/t
Adsorption constant	1.236	MPa^{-1}
True density	1.54	t/m^3
Apparent density	1.46	t/m^3
Volatiles	8.19	%
Ash content	10.04	%
Moisture content	3.84	%

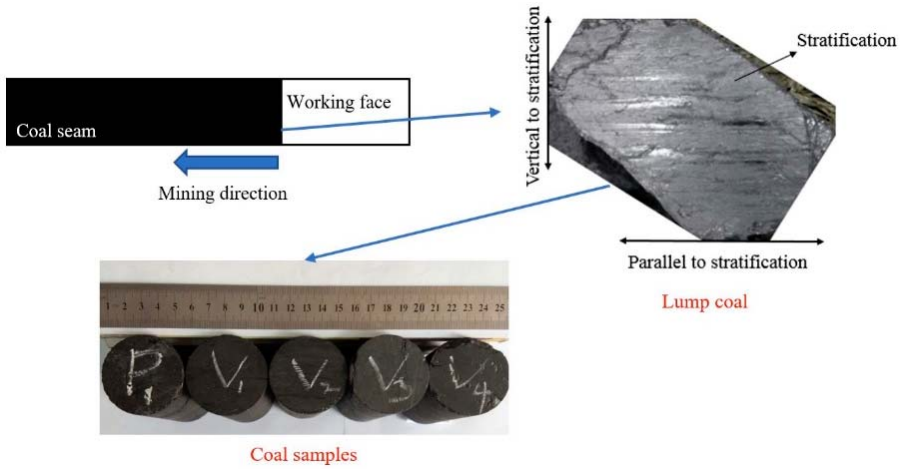Fig. 3. Preparation of coal samples

2.3. SENSITIVITY INDEX TEST

The sensitivity index of permeability to axial and confining stresses refers to the influence of axial and confining stresses on permeability. A high sensitivity index denotes a significant influence on permeability. The sensitivity index of permeability can be defined as (Geng et al. 2017)

$$S = -\frac{1}{k_0}\frac{\partial k}{\partial \sigma_{c/a}},$$ (2)

where S is the sensitivity index of permeability in MPa^{-1}, k_0 is the initial permeability of the sample in 10^{-16} m^2, k is the permeability of the sample in 10^{-16} m^2, and $\sigma_{c/a}$ is the confining or axial stress in MPa.

In this test, sample V_1 was used to study the sensitivity index of permeability to confining and axial stresses. First, confining stress (σ_c) was fixed to 1 MPa, and axial stress (σ_a) was gradually loaded from 1 to 6 MPa. Second, axial stress (σ_a) was fixed to 1 MPa, and confining stress (σ_a) was gradually loaded from 1 to 6 MPa. The inlet and outlet pressures during these processes were fixed to 0.7 and 0.1 MPa, respectively, to conduct the permeability test. Finally, the permeability index to confining and axial stresses was calculated with Eq. (2).

2.4. UNLOADING TEST

In actual mining fields, the loading of axial stress is due to the gravity of overlying strata, which indicates that axial stress is vertical to bedding planes. Hence, coal sam-

ples V_1 to V_4, which were perpendicular to the stratification, were used in this test to be consistent with the actual situation in mining fields.

In this test, the permeability of coal under different unloading paths and under the conventional loading path was compared.

1) Conventional loading path. A coal sample (V_1) was loaded in the initial state ($\sigma_a = \sigma_c = 6$ MPa). Confining stress was fixed to 6 MPa, and axial stress was gradually loaded until the coal sample was broken. The inlet and outlet pressures were fixed to 0.7 and 0.1 MPa, respectively, to conduct the permeability test. Coal permeability was calculated with Eq. (1).

2) Unloading paths. The coal samples (V_2, V_3, and V_4) were loaded in the initial state ($\sigma_a = \sigma_c = 6$ MPa). Confining stress was fixed to 6 MPa temporarily, and axial stress was gradually loaded. When the axial stress of samples V_2, V_3, and V_4 reached 10, 20, and 30 MPa, respectively, confining stress was gradually unloaded from 6 to 1 MPa. Coal permeability was tested with the same inlet and outlet pressures as those for the conventional loading path.
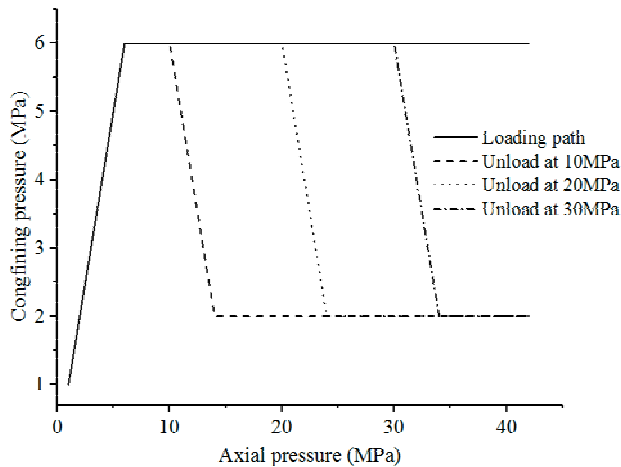
The stress paths are shown in Fig. 4.

Fig. 4. Sketch of stress paths

3. RESULTS

3.1. SENSITIVITY INDEX OF PERMEABILITY

Permeability change with axial stress can be obtained by fixing confining stress and loading axial stress, whereas permeability change with confining stress can be obtained by fixing axial stress and loading confining stress. These changes are shown

in Fig. 5a. The sensitivity index of permeability to confining and axial stresses is
shown in Fig. 5b.

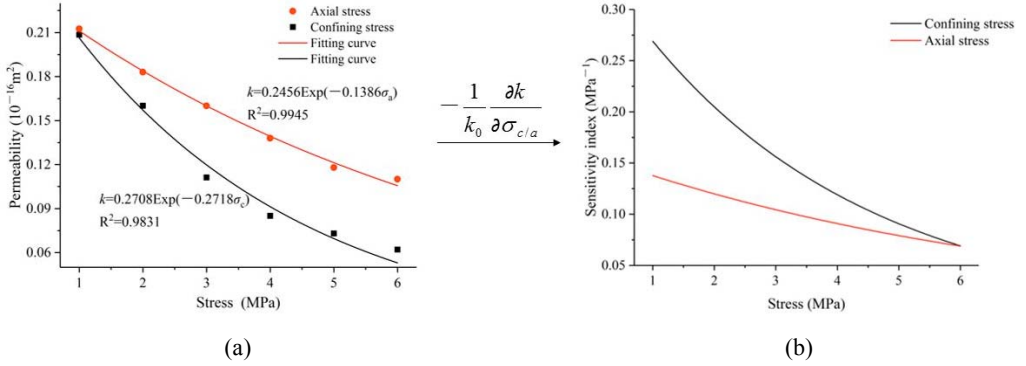(a)   (b)

Fig. 5. Calculation of the sensitivity coefficient of permeability to axial and confining stresses

Figure 5 shows that with the same change in axial and confining stresses, the de-
crease in permeability due to confining stress is more obvious that that due to axial
stress. Therefore, permeability is more sensitive to confining stress than to axial stress,
which indicates that confining stress exerts greater influence on coal permeability than
axial stress does. Moreover, the sensitivity index of permeability to axial and confin-
ing stresses was stable at high stress levels. The influence of axial and confining stress
on permeability weakened when the stress was high.

3.2. PERMEABILITY CHANGE UNDER UNLOADING CONDITIONS

Figure 6 shows the full stress–strain and stress–permeability curves of coal under load-
ing and unloading conditions. Figure 6 shows that the radial deformation, axial defor-
mation, and intensity of coal at peak strength under conventional loading conditions are
smaller than those under unloading conditions. In conventional loading, the permeability
of coal decreased gradually as the axial stress increased. Unloading confining stress
led to an increase in permeability before coal reached its peak strength. A comparative
analysis of conventional loading and unloading showed that unloading confining
stress the when axial stress was 10 MPa caused the permeability of coal to increase
from 0.0505×10^{-16} m^2 to 0.0762×10^{-16} m^2, whereas unloading confining stress when
the axial stress was 20 and 30 MPa caused the permeability of coal to increase from
0.02195×10^{-16} m^2 to 0.05×10^{-16} m^2 and from 0.01097×10^{-16} m^2 to 0.055×10^{-16} m^2,
respectively. Permeability increased by 1.51, 2.28, and 5.01 times when unloading
was at 10, 20, and 30 MPa, respectively. These results indicated that although coal
was in the stress concentration area, permeability still increased, and axial stress sig-
nificantly influenced permeability change. The larger axial stress was when unloading

confining stress, the greater the increment in permeability was during the unloading phase.

a – Loading path (V_1)

b – Unloading at 10 MPa (V_2)

c – Unloading at 20 MPa (V_3)
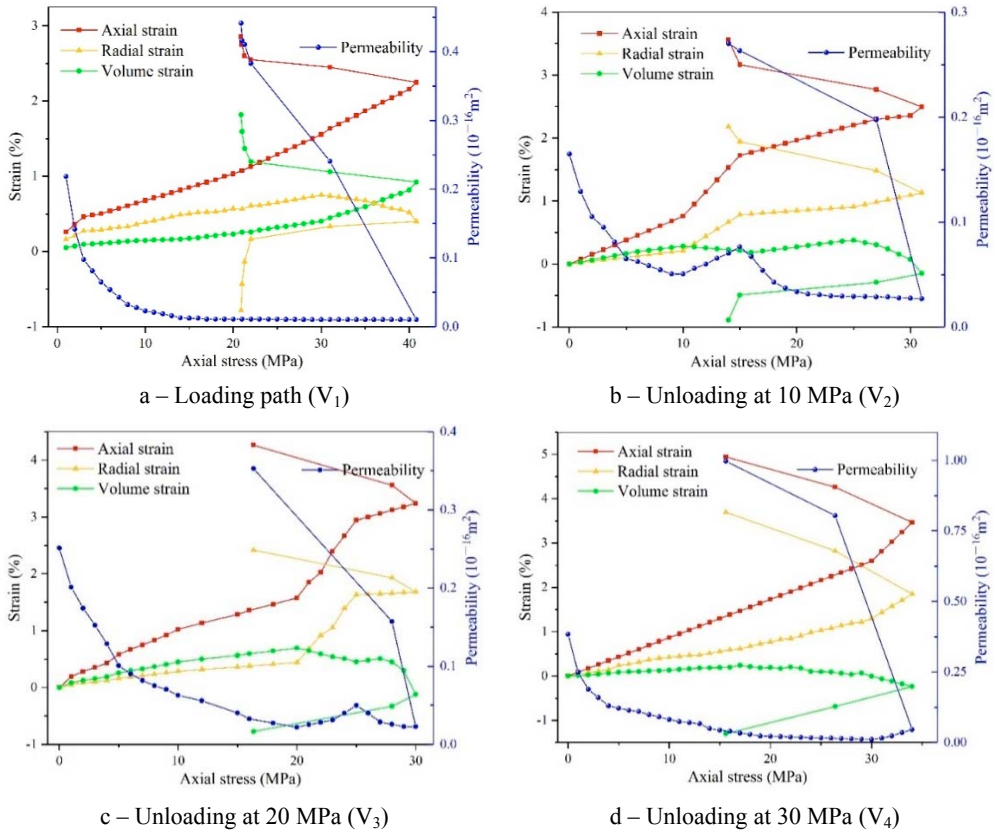
d – Unloading at 30 MPa (V_4)

Fig. 6. Full stress–strain and stress–permeability curves of coal under loading and unloading conditions

The peak strength of coal has a close relationship with confining stress, and small confining stress leads to low coal strength (Gong, Hu 2017). In the loading path in the current study (Fig. 6a), the confining stress was 6 MPa at peak strength, whereas in the unloading paths (Figs. 6b and 6c), the confining stress was 1 MPa at peak strength. Therefore, the strength of coal in the unloading paths was lower than that in the loading path. The strength of coal in the loading path was about 41 MPa, and the strength of coal in the unloading paths was about 30 MPa. However, when stress was unloaded at 30 MPa (Fig. 6d), the strength of coal was 34 MPa because coal is broken when confining stress is unloaded at 2 MPa. The unloading of confining stress provides some deformation room in the radial direction of coal and makes axial compression easy; thus, axial and radial strains in the unloading paths at peak strength were larger

than those in the conventional loading. With regard to the change in permeability, the pore space of coal was compressed, resulting in a decrease in permeability during stress loading. On the contrary, stress unloading led to an increase in permeability. However, in the unloading phase, the loading of axial stress and the unloading of confining stress coexist. The loading of axial stress leads to a decrease in permeability, whereas the unloading of confining stress leads to an increase in permeability. Permeability changes depend on the combined effect of the two aspects. At the same loading rate, the influence of confining stress on permeability is greater than that of axial stress, so permeability increases during unloading. Unloading confining stress under high axial stress indicates that permeability has low sensitivity to axial stress and high sensitivity to confining stress. Loading axial stress exerts a minimal effect on reducing coal permeability, whereas unloading confining stress exerts a significant effect on increasing coal permeability. Therefore, the increase in permeability is significant when unloading occurs at high axial stress.

4. PERMEABILITY EVOLUTION MODEL

To thoroughly understand the results, we described the modeling process of the permeability evolution model by using effective stress.

4.1. EFFECTIVE STRESS CALCULATION MODEL

In the theory of effective stress, pore pressure struts pore walls and reduces the effect of external pressure, and the effective stress can be expressed by (Helm 1987)

$$\sigma = \sigma' - \alpha p \, , \tag{3}$$

where σ is the effective stress in MPa, σ' is the external stress in MPa, α is the Boit coefficient; and p is pore pressure in MPa. Effective stress exerts a significant effect on permeability. Therefore, calculating effective stress is essential. Effective stress is highly related to axial and confining stresses. When axial and confining stresses are changed, the change in effective stress becomes the root cause of permeability evolution. To date, no direct method can be used to calculate effective stress using axial and confining stresses; instead, many studies utilized average effective stress (Zou et al. 2016; Cao et al. 2016). However, this method is inaccurate and cannot be applied to quantitative studies. To calculate effective stress using axial and confining stresses, we considered that for the same coal body, the same volume strain corresponds to the same effective stress in a certain loading range (Yin et al. 2013). This consideration is confirmed in Fig. 6 because volume strain monotonically increases when axial stress is lower than 20 MPa.
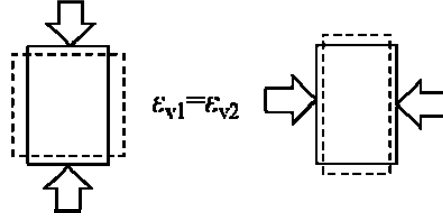
Fig. 7. Deformation diagram of the coal when loading axial and confining stresses

1. A cylindrical coal was loaded with axial stress but without confining stress and pore pressure, as shown in Fig. 7. The volumetric strain of coal caused by axial stress alone can be expressed by Eq. (4).

$$\varepsilon_{v1} = 1 - \left(1 + \frac{v\sigma_a}{E_v}\right)^2 \left(1 - \frac{\sigma_a}{E_v}\right),$$ (4)

where ε_{v1} is the volume strain of coal caused by axial stress; v is Poisson's ratio, E_v is the elastic modulus of coal that is vertical to stratification in MPa; and σ_a is the axial stress in MPa.

2. The same cylindrical coal was loaded with confining stress but without axial stress and pore pressure, as shown in Fig. 7. The volumetric strain of coal caused by confining stress alone can be expressed by Eq. (5).

$$\varepsilon_{v2} = 1 - \left(1 - \frac{\sigma_c}{E_p}\right)^2 \left(1 + \frac{\sigma_c}{vE_p}\right),$$ (5)

where ε_{v2} is the volume strain of coal caused by confining stress, v is Poisson's ratio, E_p is the elastic modulus of coal that parallel to stratification in MPa, and σ_c is the axial stress in MPa.

3. To achieve the same effective stress, the ratio of axial to confining stress was obtained when the volume strain of the two cases was the same. Considering that Eqs. (2) and (3) have $1/E^2$ and $1/E^3$, which exert little effect on the calculation results, these items were removed during the calculation process. The calculation result is as follows:

$$\frac{\sigma_c}{\sigma_a} = \frac{vE_p}{E_v}.$$ (6)

With Eq. (6), the weight of axial and confining stresses to effective stress can be obtained, and the relationship among axial, confining, and effective stresses can be expressed as

$$\sigma = \frac{E_v}{E_v + vE_p}\sigma_c + \frac{vE_p}{E_v + vE_p}\sigma_a - \alpha p.$$ (7)

4.2. PERMEABILITY EVOLUTION MODEL

Calculating permeability by using effective stress is possible because effective stress can be calculated using axial and confining stresses. Most studies have indicated that loading effective stress closes pores and leads to a decrease in porosity and permeability (Zheng et al. 2015). Conversely, unloading effective stress increases porosity and permeability. In addition, the coal matrix has a strong adsorption capacity, and the adsorption swelling of the coal matrix occupies pore space, thus causing a decrease in porosity and permeability (Chareonsuppanimit et al. 2014). When methane flows in coal, coal permeability is decided by two factors, namely, effective stress and adsorption swelling. However, in this study, the effect of adsorption swelling on permeability was unchanged because gas pressure was fixed. Therefore, effective stress plays a leading role in permeability change.

Previous studies have found that volume change in coal caused by effective stress is almost equal to pore volume change (Ettinger 1979), indicating that effective stress exerts more effect on the pore than on the matrix and that the volume deformation of the coal matrix is minimal. A permeability evolution model was built based on this analysis, and the modeling procedures were as follows.

1. Volume deformation of entire coal

Coal volume deformation is expanded because adsorption swelling of the coal matrix may cause a small change in coal volume, leading to a change in external stress. However, this expansion in coal volume deformation is minimal and can be disregarded in low-gas-pressure or high-external-stress conditions (Liu et al. 2017). The average gas pressure was only 0.4 MPa in this study. Thus, the adsorption swelling of the coal matrix was mostly internal expansion and led to a greater change in pore volume than in coal volume. Hence, we conclude that volume deformation of coal is mostly caused by effective stress, a change in effective stress leads to volume deformation of the entire coal. This volume deformation can be calculated with Eq. (8).

$$K = \frac{1}{V}\frac{dV}{d\sigma},\qquad(8)$$

where K is the volumetric compressibility coefficient in MPa^{-1}, V is the volume of coal under stress in cm^3, and σ is the effective stress in MPa. Coal volume under stress was then obtained by using Eq. (8).

$$V = V_{c0}e^{-K\Delta\sigma},\qquad(9)$$

where V_{c0} is the initial volume of coal in cm^3 and $\Delta\sigma$ is the increment in effective stress in MPa. The volumetric strain of coal caused by effective stress can be described by Eq. (10).

$$\varepsilon_v = \frac{V - V_{c0}}{V_{c0}} = \frac{V}{V_{c0}} - 1 = e^{-K\Delta\sigma} - 1. \tag{10}$$

2. Pore volume deformation

Effective stress and adsorption swelling are the factors that affect pore volume deformation. Pore volume change caused by effective stress is equal to volume change in coal and can be expressed by Eq. (10). Pore volume change caused by adsorption swelling can be described with adsorption strain (Pan, Connell 2007).

$$\varepsilon_p = \frac{\rho_v}{E_s} \int_0^p \frac{N_a RT}{pV_m} dp, \tag{11}$$

where ε_p is the adsorption strain, ρ_v is the apparent density of coal in kg/m³, E_s is the solid elastic modulus of coal in Pa, R is the gas constant in J/(mol·K), T is temperature in K, p is adsorption pressure (average gas pressure) in Pa, and V_m is the molar volume of gas in m³/mol, N_a is adsorbed methane content, which can be calculated with the Langmuir equation.

$$N_a = \frac{V_L bp}{1 + bp}, \tag{12}$$

where V_L is the Langmuir equilibrium constant (adsorption capacity) in m³/kg and b is the adsorption constant in Pa^{-1}. By incorporating Eq. (12) into Eq. (11) and evaluating the integral, adsorption strain can be obtained and expressed as Eq. (13).

$$\varepsilon_p = -\frac{\rho_v V_L RT}{E_s V_m} \ln(1 + bp). \tag{13}$$

3. Permeability evolution model

According to the volume of coal and pores, porosity can be calculated as

$$\varphi = \frac{V_p}{V_c} = \frac{V_{p0} + \Delta V_{p1} + \Delta V_{p2}}{V_{c0} + \Delta V_c}$$

$$= \frac{\left(V_{p0} + \Delta V_{p1} + \Delta V_{p2}\right)/V_{c0}}{\left(V_{c0} + \Delta V_c\right)/V_{c0}} = \frac{\varphi_0 + \varepsilon_v + \varepsilon_p}{1 + \varepsilon_v} l, \tag{14}$$

where φ is porosity, V_p is the volume of pores, V_c is the volume of coal, V_{p0} is the initial volume of pores, ΔV_{p1} is the pore volume change caused by effective stress, ΔV_{p2} is the pore volume change caused by adsorption swelling, V_{c0} is the initial volume of coal, and ΔV_c is the volume change of coal.

According to the Kozeny–Carman equation (Seidle, Huitt 1995), porosity and permeability have the following relationship.

$$\frac{k}{k_0} = \left(\frac{\varphi}{\varphi_0}\right)^3 . \tag{15}$$

Finally, a dynamic evolution model of permeability is established as follows:

$$k = k_0 \left(\frac{\varphi_0 + e^{-K\Delta\sigma} - 1 - \dfrac{\rho_v V_L RT}{E_s V_m}\ln(1+bp)}{\varphi_0 e^{-K\Delta\sigma}}\right)^3, \tag{16}$$

where k_0 is the initial permeability.

4.3. MODEL PARAMETERS

Most model parameters, such as elastic moduli E_v, E_p, and E_s, Poisson's ratio v, adsorption capacity V_L, adsorption constant b, and apparent density ρ, can be acquired easily through experimental tests. However, further tests are required to acquire initial porosity φ_0, initial permeability k_0, and volumetric compressibility coefficient K. The sample marked as V_2 was regarded as an example to obtain these parameters.

1. Initial porosity and permeability

An iron cylinder with a round ostiole in the center was used to measure initial porosity, as shown in Fig. 8. This iron cylinder was placed in the sample holder, the system was filled with pressured gas, pressure was released, and the released gas was collected by the flowmeter. In this manner, the fixed volume of the experimental system was calibrated. Next, the coal sample marked as V_2 was placed in the sample holder instead of the iron cylinder, and the experimental system was degassed using a vacuum pump. The system was loaded with pressured helium gas, which cannot be adsorbed by coal. The pressure was maintained for 24 h and then released. The released gas was also collected by the flowmeter. Porosity was calculated with the following equations:

$$(V_s + V_i)p_1 = Q_1 p_0,$$
$$(V_s + V_{p0})p_2 = Q_2 p_0, \tag{17}$$
$$\varphi_0 = \frac{V_{p0}}{V_{c0}},$$

where V_s is the fixed volume of the experimental system, V_i is the volume of the micro-void in the iron cylinder, p_1 and p_2 are the gas pressure used for calibrating the

fixed volume and for measuring porosity, respectively; and Q_1 and Q_2 are the gas contents used for calibrating the fixed volume and for measuring porosity, respectively.
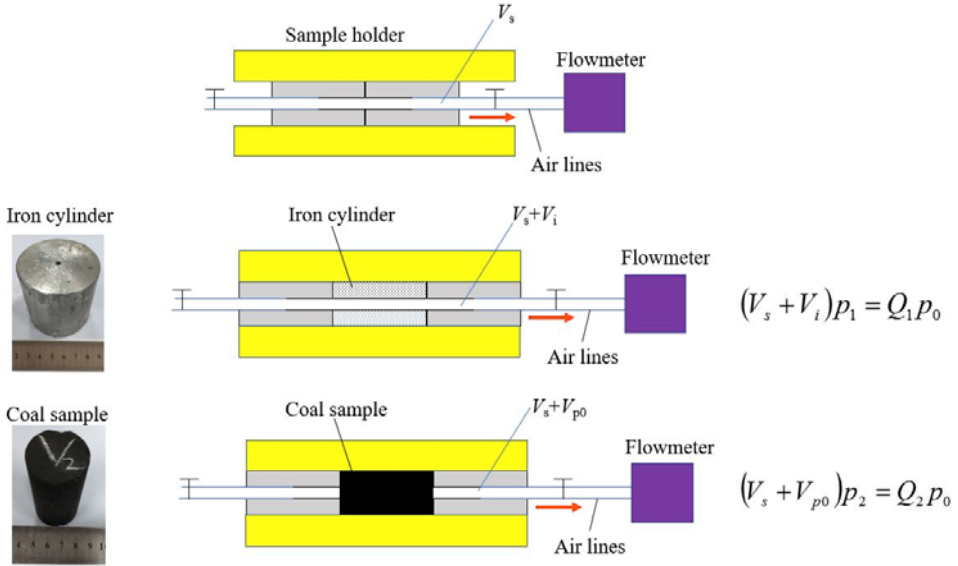

Fig. 8. Process of measuring initial porosity

Initial permeability was easily determined by using helium and fixing the inlet and outlet pressures to 0.7 and 0.1 MPa, respectively.

2. Volumetric compressibility coefficient

Considering that effective stress can be calculated using axial and confining stresses, the relation between effective stress and volume strain can be obtained with the experimental data on volume strain in Fig. 6b. The volumetric compressibility coefficient can be easily obtained with Eq. (8). The model parameters are shown in Table 2.

Table 2. Basic physical parameters of the coal sample

Parameters	Value	Unit	Parameters	Value	Unit
Initial permeability	0.1846	10^{-16} m^2	Initial porosity	3.96	%
Average gas pressure	0.4	MPa	Poisson's ratio	0.28	
Gas constant	8.3143	J/(mol·K)	Elastic modulus E_p	3365	MPa
Molar volume	0.0224	m^3/mol	Elastic modulus E_v	2672	MPa
Boit coefficient	0.875		Elastic modulus E_s	4632	MPa
Volumetric compressibility coefficient	2.059×10^{-3}	MPa^{-1}	Temperature	298.15	K

4.4. MODEL VALIDATION

When axial and confining stresses are the same, external stress is equal to axial or confining stress. Hence, effective stress under this condition can be obtained easily. When axial and confining stresses are different, effective stress is calculated with Eq. (7). Although different methods are used to load effective stress, the permeability of the same coal presents a similar change as effective stress, and the effective stress calculation model can be verified according to this characteristic. In the experiments, coal sample V_1 was used in the sensitivity and conventional loading tests. Effective stress was calculated under three loading conditions by using the data in Figs. 4a and 5a. The results are shown in Table 3, and the permeability change with effective stress is shown in Fig. 9. Figure 9 shows that the three curves nearly coincide, indicating that the effective stress calculated using Eq. (7) is close to the actual effective stress. Therefore, calculating the effective stress using Eq. (7) is accurate. In addition, the weight of confining stress in effective stress is 0.6944, whereas the weight of axial stress is 0.3056. This result indicates that loading axial stress and unloading confining stress at the same time led to a decrease in effective stress. Therefore, permeability increased during unloading.

Table 3. Effective stress calculated in three loading conditions

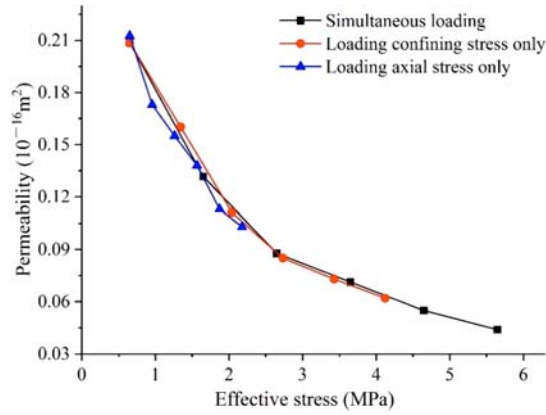| Loading conditions	Axial stress (MPa)	Confining stress (MPa)	Effective stress (MPa)	Permeability (mD)
Simultaneous loading of axial and confining stress	1	1	0.65	0.2085
	2	2	1.65	0.1317
	3	3	2.65	0.0878
	4	4	3.65	0.0713
	5	5	4.65	0.0549
	6	6	5.65	0.0439
Loading confining stress only	1	1	0.65	0.2085
	1	2	1.3444	0.1601
	1	3	2.0388	0.1112
	1	4	2.7332	0.085
	1	5	3.4276	0.73
	1	6	4.122	0.062
Loading axial stress only	1	1	0.65	0.2085
	2	1	0.9556	0.173
	3	1	1.2612	0.16
	4	1	1.5668	0.138
	5	1	1.8724	0.113
	6	1	2.178	0.103

Fig. 9. Change in permeability with effective stress under three loading conditions
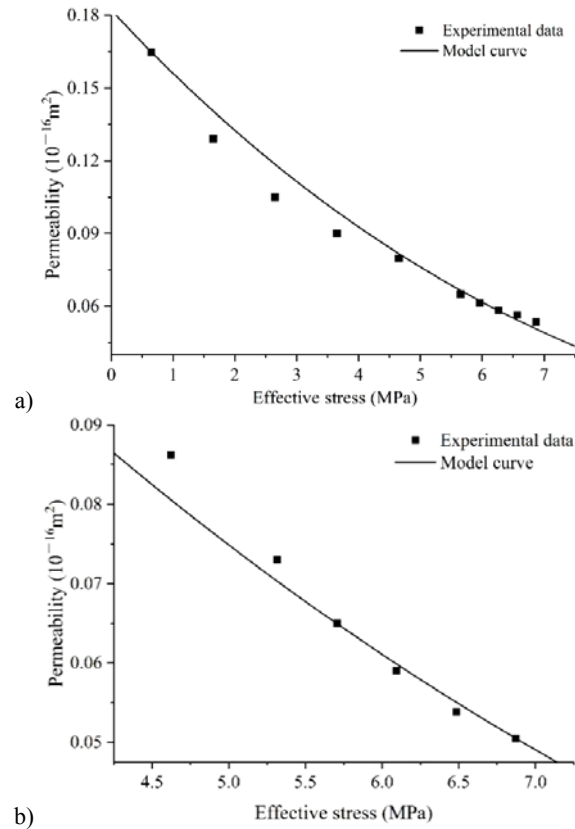

a)

b)

Fig. 10. Comparison of the model curve and experimental data:
(a) comparison of the model curve and experimental data in the loading phase,
(b) comparison of the model curve and experimental data in the unloading phase

The established permeability evolution model was solved with the parameters in Table 2 to verify the model. After the completion of the loading phase, the data at the end of the loading phase were regarded as the initial data of the unloading phase. In this manner, the relationship between the permeability of coal and effective stress was obtained. A comparison of the calculated results with the experimental data in Fig. 6b is shown in Fig. 10. The fitting correlations between the calculated and experimental results were 0.9916 and 0.9811. Thus, the model calculation result was basically consistent with the experimental data and could well describe the permeability evolution of coal in the stress concentration region.

5. CONCLUSIONS

We conducted experiments to study the changes in permeability when axial stress is loaded and confining stress is unloaded. The sensitivity of permeability to axial and confining stresses was studied. We built two models to illustrate permeability evolution under unloading paths. The main conclusions are as follows.

1. Unloading paths demonstrated lower strength and larger axial and radial strains than the loading path. When coal gradually entered the stress concentration region from the original state, coal permeability began to increase, and the increment was enlarged with the increase in axial stress at the unloading point.

2. The permeability sensitivity index to confining and axial stresses was used to explain permeability change when loading axial stress and unloading confining stress simultaneously. Coal permeability was more sensitive to confining stress than to axial stress. Therefore, the unloading of confining stress was the main factor that controlled permeability and led to an increase in permeability in stress concentration region.

3. The weight of axial and confining stresses in effective stress was obtained based on the influence of axial and confining stresses on volume deformation. We also built a model to calculate effective stress using axial and confining stresses. The results showed that confining stress had a large weight in effective stress, which led to a decrease in effective stress when axial stress loading and confining stress unloading occurred at the same time.

4. Permeability change is highly related to effective stress. Through an analysis of the volume change in the coal and pores under effective stress and adsorption swelling, a permeability evolution model was built and verified with the experimental data. The model fitted the experimental data well and showed sufficient accuracy to describe the evolution of coal permeability in the stress concentration region.

ACKNOWLEDGMENTS

REFERENCES

CAO P., LIU J., LEONG Y.K., 2016, *Combined impact of flow regimes and effective stress on the evolution of shale apparent permeability*, Journal of Unconventional Oil and Gas Resources, 14, 32–43. DOI: 10.1016/j.juogr.2016.01.004.

CHAREONSUPPANIMIT P., MOHAMMAD S.A., ROBINSON R.L., GASEM K.A., 2014, *Modeling gas-adsorption-induced swelling and permeability changes in coals*, International Journal of Coal Geology, 121, 98–109, DOI: 10.1016/j.coal.2013.11.009.

CHEN D., PAN Z., LIU J., CONNELL L.D., 2012, *Characteristic of anisotropic coal permeability and its impact on optimal design of multi-lateral well for coalbed methane production*, Journal of Petroleum Science and Engineering, 88, 13–28, DOI: 10.1016/j.petrol.2012.04.003.

CHEN J., JIANG D., REN S., YANG C., 2016a, *Comparison of the characteristics of rock salt exposed to loading and unloading of confining stress*, Acta Geotechnica, 11 (1), 221–230, DOI: 10.1007/s11440-015-0369-9.

CHEN J., DU C., JIANG D., FAN J., HE Y., 2016b, *The mechanical properties of rock salt under cyclic loading-unloading experiments*, Geomechanics and Engineering, 10 (3), 325–334, DOI: 10.12989/gae.2016.10.3.325

CONG L., HU X., 2017, *Triaxial rheological property of sandstone under low confining stress*, Engineering Geology, 231, 45–55, DOI: 10.1016/j.enggeo.2017.10.005.

DENG T., TANG J.X., CHEN J., 2012, *Experiment study of mechanical and gas seepage characteristics of containing-gas coal in the process of unloading confining pressure*, Advanced Materials Research, 524–527, 297–301, DOI: 10.4028/www.scientific.net/AMR.524-527.297.

ETTINGER I.L., 1979, *Swelling stress in the gas-coal system as an energy source in the development of gas bursts*, Journal of Mining Science, 15 (5), 494–501, DOI: 10.1007/BF02499473.

GENG Y., TANG D., XU H., TAO S., TANG S., MA L., ZHU X., 2017, *Experimental study on permeability stress sensitivity of reconstituted granular coal with different lithotypes*, Fuel, 202, 12–22, DOI: 10.1016/j.fuel.2017.03.093.

HELM D.C., 1987, *Three-dimensional consolidation theory in terms of the velocity of solids*, Geotechnique, 37 (3), 369–392, DOI: 10.1680/geot.1987.37.3.369.

HUANG B., LIU J., 2013, *The effect of loading rate on the behavior of samples composed of coal and rock*, International Journal of Rock Mechanics and Mining Sciences, 61, 23–30, DOI: 10.1016/j.ijrmms.2013.02.002.

JASINGE D., RANJITH P.G., CHOI S.K., 2011, *Effects of effective stress changes on permeability of latrobe valley brown coal*, Fuel, 90 (3), 1292–1300, DOI: 10.1016/j.fuel.2010.10.053.

JIANG C., YIN G., LI W., HUANG Q., 2011, *Experimental of mechanical properties and gas flow of containing-gas coal under different unloading speeds of confining stress*, Procedia Engineering, 26, 1380–1384, DOI: 10.1016/j.proeng.2011.11.2314.

LI Y., TANG D., XU H., MENG Y., LI J., 2014, *Experimental research on coal permeability: the roles of effective stress and gas slippage*, Journal of Natural Gas Science and Engineering, 21, 481–488, DOI: 10.1016/j.jngse.2014.09.004.

LIU T., LIN B., YANG W., 2017, *Impact of matrix–fracture interactions on coal permeability: Model development and analysis*, Fuel, 207, 522–532, DOI: 10.1016/j.fuel.2017.06.125.

MENG J., NIE B., ZHAO B., MA Y., 2015, *Study on law of raw coal seepage during loading process at different gas pressures*, International Journal of Mining Science and Technology, 25 (1), 31–35, DOI: 10.1016/j.ijmst.2014.12.005.

PAN Z., CONNELL L.D., 2007, *A theoretical model for gas adsorption-induced coal swelling*, International Journal of Coal Geology, 69 (4), 243–252, DOI: 10.1016/j.coal.2006.04.006.

SEIDLE J.R., HUITT L.G., January 1995, *Experimental measurement of coal matrix shrinkage due to gas desorption and implications for cleat permeability increases*. [In:] International Meeting on Petroleum Engineering, Society of Petroleum Engineers, DOI: 10.2118/30010-MS.

SHEN W., BAI J., LI W., WANG X., 2018, *Prediction of relative displacement for entry roof with weak plane under the effect of mining abutment stress*, Tunnelling and Underground Space Technology, 71, 309–317, DOI: 10.1016/j.tust.2017.08.023.

TIAB D, DONALDSON E.C., 2016, Chapter 7 – *Applications of Darcy's Law*. [In:] *Petrophysics* (Fourth Edition), Gulf Professional Publishing, Boston, pp. 359–414, DOI: 10.1016/B978-075067711-0/50011-6.

XIE H., ZHOU H., LIU J., XUE D., 2011, *Mining-induced mechanical behavior in coal seams under different mining layouts*, Journal of China Coal Society, 36 (7), 1067–1074, DOI: 10.13225/j.cnki.jccs.2011.07.025.

XUE Y., RANJITH P.G., GAO F., ZHANG D., CHENG H., CHONG Z., HOU P., 2017, *Mechanical behaviour and permeability evolution of gas-containing coal from unloading confining stress tests*, Journal of Natural Gas Science and Engineering, 40, 336–346, DOI: 10.1016/j.jngse.2017.02.030.

YIN G., JIANG C., WANG J.G., XU J., 2015, *Geomechanical and flow properties of coal from loading axial stress and unloading confining stress tests*, International Journal of Rock Mechanics and Mining Sciences, (76), 155–161, DOI: 10.1016/j.ijrmms.2015.03.019.

YIN G., LI W., JIANG C., LI M., LI X., LIU H., ZHANG Q., 2013, *Mechanical property and permeability of raw coal containing methane under unloading confining stress*, International Journal of Mining Science and Technology, 23 (6), 789–793, DOI: 10.1016/j.ijmst.2013.10.002.

YIN G., LI W., LI M., DENG B., JIANG C., 2014, *Permeability properties and effective stress of raw coal under loading-unloading conditions*, Journal of China Coal Society, 39 (8), 1497–1503, DOI: 10.13225/j.cnki.jccs.2014.9011.

ZHANG Z., ZHANG R., XIE H., GAO M., ZHA E., JIA Z., 2017, *An anisotropic coal permeability model that considers mining-induced stress evolution, microfracture propagation and gas sorption-desorption effects*, Journal of Natural Gas Science and Engineering, 46, 664–679, DOI: 10.1016/j.jngse.2017.08.028.

ZHANG L., ZHANG H., GUO H., 2017, *A case study of gas drainage to low permeability coal seam*, International Journal of Mining Science and Technology, 27, 687–692, DOI: 10.1016/j.ijmst.2017.05.014.

ZHAO H., WANG J., 2011, *Experimental study of evolution law of mechanical properties of coal containing gas under unloading confining stress*, Rock Soil Mechanics, 32 (Suppl. 1), 270–274, DOI: 10.16285/j.rsm.2011.s1.029.

ZHENG J., ZHENG L., LIU H.H., JU Y., 2015, *Relationships between permeability, porosity and effective stress for low-permeability sedimentary rock*, International Journal of Rock Mechanics and Mining Sciences, 78, 304–318, DOI: 10.1016/j.ijrmms.2015.04.025.

ZOU J., CHEN W., YANG D., YU H., YUAN J., 2016, *The impact of effective stress and gas slippage on coal permeability under cyclic loading*, Journal of Natural Gas Science and Engineering, 31, 236–248, DOI: 10.1016/j.jngse.2016.02.037.